Appendix DR1

This file contains additional information accompanying the manuscript by M. Portnyagin and V. Manea "Mantle temperature control on composition of arc magmas along the Central Kamchatka Depression" (Geology, 2008)

NUMERIC MODELING PROCEDURE

A system of 2D Navier-Stokes equations and 2D steady state heat transfer equation are solved using the numerical scheme proposed by Manea et al. (2005). Below we present a short description of the numerical model setup.

The strong temperature-dependence of viscosity imposed in the present modeling, corresponding to diffusion creep of olivine, has the following form:

$$\eta = \eta_0 \cdot \mathrm{e}^{\left[\frac{E_a}{R \cdot T_0} \cdot \left(\frac{T_0}{T} - 1\right)\right]}$$

The system of equations in an explicit form is:

$$\begin{cases} \dfrac{\partial\left(-P + 2\eta\dfrac{\partial u}{\partial x}\right)}{\partial x} + \dfrac{\partial\left(\eta\left(\dfrac{\partial u}{\partial y} + \dfrac{\partial v}{\partial x}\right)\right)}{\partial y} = 0 \\ \dfrac{\partial\left(\eta\left(\dfrac{\partial u}{\partial y} + \dfrac{\partial v}{\partial x}\right)\right)}{\partial x} + \dfrac{\partial\left(-P + 2\eta\dfrac{\partial v}{\partial y}\right)}{\partial y} = -\rho \cdot g - Ra \cdot T \\ C_p\left(u\dfrac{\partial T}{\partial x} + v\dfrac{\partial T}{\partial y}\right) = \dfrac{\partial}{\partial x}\left(k\dfrac{\partial T}{\partial x}\right) + \dfrac{\partial}{\partial y}\left(k\dfrac{\partial T}{\partial y}\right) + Q + Q_{sh} \end{cases}$$

The parameters used are:

η_0	-mantle wedge viscosity at the potential temperature T_0 (reference viscosity = 10^{20} Pa s),
T_0	-mantle wedge potential temperature (1,350ºC),
Ea	-activation energy for olivine (300 kJ/mol) (Karato and Wu, 1993),
R	-universal gas constant (8.31451 J/mol.K),
T	-temperature (ºC),
u	-horizontal component of the velocity (m/s),
v	-vertical component of the velocity (m/s),
ρ	-density (kg/m^3),
C_p	-thermal capacity (MJ/m^{3}K),
k	-thermal conductivity (MJ/m^{3}K),
Q	-radiogenic heating (W/m^3),
Q_{sh}	-volumetric shear heating (W/m^3),
$Ra = \dfrac{\rho \cdot \alpha \cdot g \cdot \Delta T \cdot L^3}{\eta_0 \cdot k}$	-thermal Rayleigh number,
α	-thermal expansion $3.5 \cdot 10^{-5}$ (1/ºC),
L	-length scale (350 km),
ΔT	-temperature difference between the bottom and top model

temperatures (1,350 ºC),
k -thermal diffusivity (10^{-6} m/s^2),
g -gravitational acceleration (9.81 m/s^2).

A computational domain is 370 km x 300 km, and consists of 12,000 triangular elements with an average mesh resolution of 5 km. The lower edge of the grid follows the shape of the subducting plate upper surface at a constant distance of 100 km. The model consists of five thermo-stratigraphic units: upper continental crust (0 - 15 km depth), lower continental crust (15 - 35 km depth), oceanic crust (10 km-thick), oceanic sediments (1.5 km-thick), oceanic lithosphere and mantle wedge. A summary of the thermal parameters used is presented in Manea et al. (2005). The shape and dip of the subducting plate beneath the volcanic arc are constrained by earthquake hypocenter distribution. The upper and lower boundaries are maintained at constant temperatures of 0ºC at surface and of 1,350ºC in the asthenosphere. The left, landward vertical boundary condition is defined by a 23ºC/km thermal gradient for the continental crust. Below the Moho (35 km depth), the left boundary condition is represented by a low thermal gradient of 8.5ºC/km down to the depth of 100 km. Beneath 100 km depth no horizontal conductive heat flow is specified. Underneath the Moho (35 km), for the left boundary, corresponding to the mantle wedge, zero traction is assumed. The right, seaward boundary condition is a one-dimensional geotherm calculated for the oceanic plate by allowing a half-space to cool from zero age to the Pacific oceanic plate age at the trench (84 Ma). In terms of displacement, the velocity of the oceanic plate is taken with respect to the continental plate. We used a convergence rate of 7.4-7.5 cm/year between the Pacific plate and Kamchatka (Renkin and Sclater, 1988). We also introduced into the models a small degree of frictional heating along the plate interface down to a depth of 35 km (Byerlee, 1978). Volumetric shear heating is calculated as follows:

$$Q_{sh} = \frac{\tau \cdot v}{w} \quad ,$$

where:

Q_{sh} -volumetric shear heating (mW/m^3),

τ -shear stress:
$$\tau = 0.85 \cdot \sigma_n \cdot (1-\lambda) \quad for \quad \sigma_n \cdot (1-\lambda) \le 200 MPa$$
$$\tau = 50 + 0.6 \cdot \sigma_n \cdot (1-\lambda) \quad for \quad \sigma_n \cdot (1-\lambda) > 200 MPa \quad ,$$

σ_n -lithostatic pressure (MPa),
λ -the pore pressure ratio, (the ratio between the hydrostatic and lithostatic pressures ($0 \le \lambda \le 1$). The maximum value, $\lambda = 1$, means no frictional heating),
V -convergence velocity (7.4-7.5 cm/year),
W -the thickness of a thin element layer (500 m) along the plate-interface, where frictional heating is formulated as body-heat source.

REFERENCES

Arculus, R.J., 2003, Use and abuse of the terms calcalkaline and calcalkalic: Journal of Petrology, v. 44, p. 929-935.

Byerlee, J.D., 1978. Friction of rocks. Pure Applied Geophysics, v. 116, p. 615-626.

Karato, S., and Wu, P., 1993. Rheology of the upper mantle: a synthesis. Science v. 260, p. 771–778.

Kelley, K., Plank, T., Grove, T.L., Stolper, E.M., Newman, S., and Hauri, E., 2006, Mantle melting as a function of water content beneath back-arc basins, Journal of Geophysical Research, v. 111, B09208, doi:10.1029/2005JB003732.

Manea, V.C., Manea, M., Kostoglodov, V., and Sewell, G., 2005, Thermo-mechanical model of the mantle wedge in Central Mexican subduction zone and a blob tracing approach for the magma transport: Physics of the Earth and Planetary Interiors, v. 149, p. 165-186.

Manea, V.C., and Manea, M., 2007, Thermal Models Beneath Kamchatka and the Pacific Plate Rejuvenation From a Mantle Plume Impact, *in* Eichelberger, J., Gordeev, E., Kasahara, M., Izbekov, P., and Lees, J., eds., Volcanism and Subduction: The Kamchatka Region, Volume 172: Washington D.C., American Geophysical Union, p. 81-94.

Miyashiro, A., 1974, Volcanic rock series in island arcs and active continental margins: American Journal of Science, v. 274, p. 321-355.

Renkin, M.L., and Sclater, J.G., 1988, Depth and age in the North Pacific. Journal of Geophysical Research, v. 93, B4, p. 2919-2935.

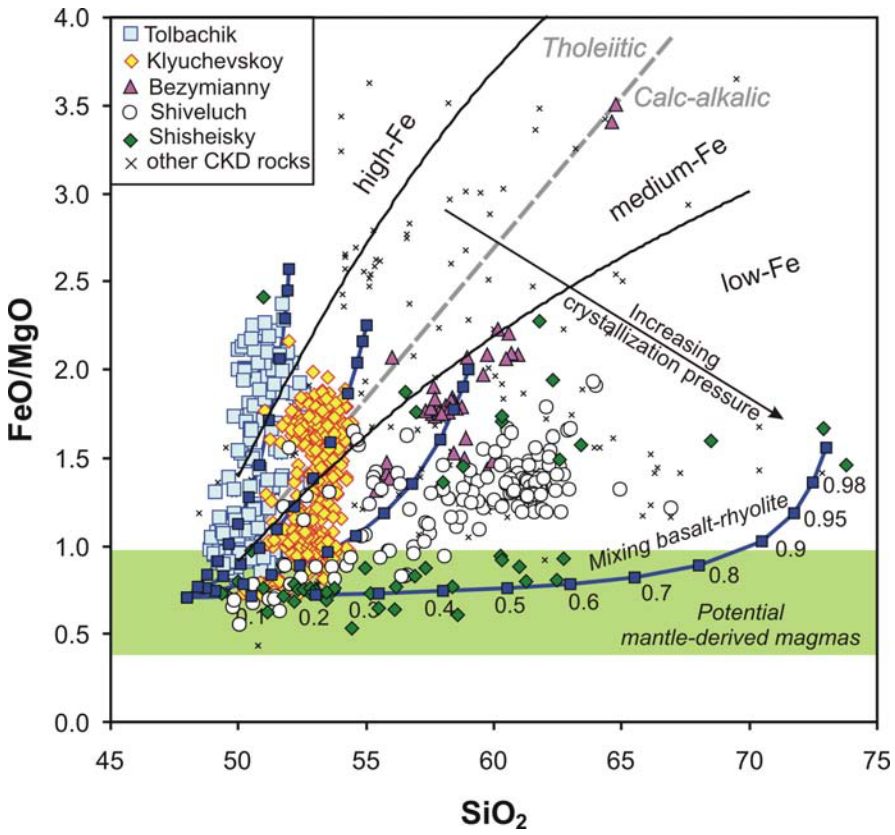

Figure DR1. SiO_2 versus FeO/MgO diagram (FeO refers to total Fe). Fields of tholeiitic and calc-alkaline series (Miyashiro, 1974) and high-Fe, middle-Fe and low-Fe (Arculus, 2003) are shown for comparison. Field of potential mantle-derived magmas includes compositions in equilibrium with mantle olivine Fo89-93 (assuming distribution coefficient Fe-Mg between olivine and melt to be 0.3). Bold blue curves illustrate a range of composition resulted from mixing of primitive mantle-derived melt (SiO_2=48 wt%, FeO=8.5 wt%, MgO=12 wt%) and evolved melts ranging from rhyolite (lower curve) to high-Al basalt (upper curve). Squares along the mixing trends indicate the amount (mass fraction) of evolved end-member in the mixture as labeled along the lower curve. Note that all mixing trends are concave in these coordinates. Therefore, mixing of primitive and evolved magmas is able to generate high-magnesian magma compositions of substantial range of SiO_2 content, much exceeding that of true parental magma. An effect of increasing crystallization pressure is shown by arrow. Low pressure crystal fractionation is dominated by olivine, plagioclase and pyroxene assemblage, whereas amphibole becomes more important at increasing pressure, which results in strong silica enrichment at moderate increase of FeO/MgO in evolved melts.

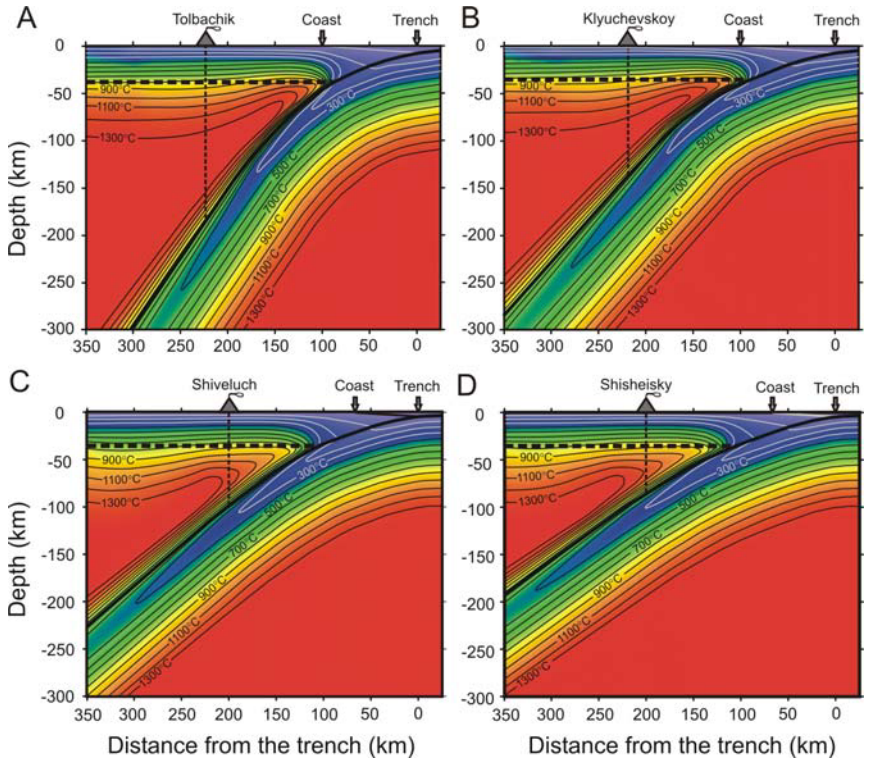

Figure DR2. Numeric thermal models for CKD. (A-D) trench normal cross-sections for Tolbachik, Klyuchevskoy, Shiveluch and Shisheisky Complex, respectively. The models were calculated as described in the Supplementary Methods. These models and the slab edge thermal structure from (Manea et al. 2007) were used to constrain trench-parallel along-arc section shown in Figure 3A of the manuscript.

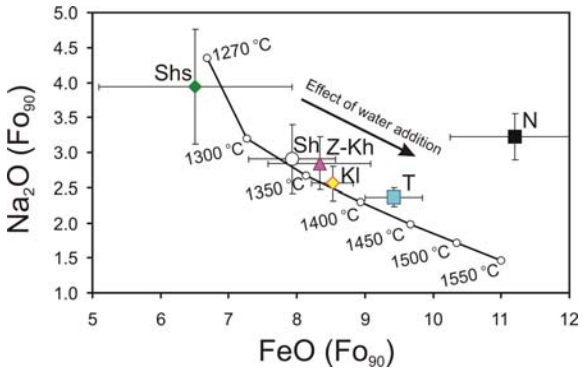

Figure DR3. Mean compositions of primitive (Mg#>0.65) CKD rocks. Aggregate fractional melts with H_2O<0.5 wt% originated at different potential mantle temperatures (Tp) are after Kelley et al. (2006). Effect of water on magma composition at fixed Tp, which results in lower Na_2O and higher FeO due to increasing degree of melting and mean melting pressure, is shown by arrow. Volcano abbreviations: T – Tolbachik, KL – Klyuchevskoy, Z-Kh – Zarechny and Kharchinsky volcanoes, Sh – Shiveluch, Shs – Shisheisky Complex; N – Nachikinsky. Note deviation of the composition of primitive melts of Nachikinsky volcano from the general trend of CKD rocks, which indicates different conditions of magma generation further to the north from the subducting slab edge.

Table DR1. Mean compositions of CKD primitive rocks

Volcano	Tolbachik		Klyuchevskoy		Zarechny & Kharchinsky		Shiveluch		Shisheisky Complex	
Latitude (degrees North)	55.7		56.1		56.4		56.6		57.4	
Longitude (degrees East)	160.3		160.6		160.8		161.3		161.3	
Slab depth (km)	190		160		140		90		80 (?)	
Distance from slab edge (km)	170		140		100		60		0	
Mantle collumn (km)	155		125.0		105		55		45 (?)	
Primitive rocks (Mg#>0.65)										
Number of analyses	38		70		24		31		33	
	Mean	1 s.d.	Mean	1 s.d.	Mean	1 s.d.	Mean	1 s.d.	Mean	1 s.d.
SiO_2 (wt%)	50.1	0.7	52.0	0.9	51.4	1.3	52.9	2.3	55.2	3.7
TiO_2(wt%)	1.01	0.12	0.84	0.06	0.84	0.08	0.78	0.18	0.68	0.13
Al_2O_3 (wt%)	13.5	0.5	14.1	0.6	13.3	1.1	14.3	1.1	15.3	0.9
FeO t (wt%)	9.4	0.4	8.5	0.3	8.3	0.7	7.9	0.6	6.5	1.4
MnO (wt%)	0.18	0.02	0.17	0.01	0.17	0.02	0.15	0.02	0.12	0.03
MgO (wt%)	10.3	0.5	10.5	1.2	11.5	2.5	10.2	2.1	8.8	2.4
CaO (wt%)	11.3	0.9	9.7	0.4	8.6	1.0	8.1	0.7	6.9	1.5
Na_2O (wt%)	2.36	0.13	2.56	0.25	2.84	0.38	2.91	0.49	3.94	0.82
K_2O (wt%)	0.95	0.18	0.73	0.14	1.35	0.59	1.35	0.37	1.12	0.27
P_2O_5 (wt%)	0.23	0.06	0.15	0.03	0.25	0.07	0.27	0.13	0.18	0.08
Tp (^oC) dry *	1434	29	1375	19	1364	43	1339	37	1268	67
SiO_2 (wt%) @ X_e=30% $	55		61		59		64		72	
Xe (wt%) @ SiO_2 (e)=72 wt%&	0.09		0.17		0.14		0.20		0.30	
Compositions at MgO=6 wt%#										
Si_6 (wt%)	50.7		53.1		55.5		55.9		56.8	
Ti_6(wt%)	1.37		1.00		0.80		0.70		0.60	
Al_6 (wt%)	16.1		17.1		15.5		16.0		16.0	
Fe_6 (wt%)	9.9		8.5		7.0		6.7		5.7	
Ca_6 (wt%)	9.3		8.6		7.7		7.7		6.0	
Na_6 (wt%)	3.1		3.2		3.6		3.5		4.5	
K_6 (wt%)	1.60		1.00		1.84		1.30		1.20	

Notes:

* Apparent 'dry' potential mantle temperature (Tp) calculated from FeO content in primitive rocks using parametrization from Kelley et al. (2006).

$ Estimated concentration of SiO_2 in evolved magma beneath volcanoes assuming that the mean compositions of primitive rocks are mixtures of mantle-derived basalt (SiO_2=48 wt%) and 30% of evolved magma.

& Estimated mass fraction of evolved melt with SiO_2=72 wt%, which is required to explain SiO_2 in the mean composition of primitive rocks, if this evolved melt mixed with mantle-derived magma (SiO_2=48 wt%). Note that the model of the origin of primitive rocks by mixing with evolved magmas requires either volcano-specific evolved end-member or systematically increasing contribution from evolved magma of constant SiO_2 content from south to north along the CKD.

Concentrations of oxides in rock series at MgO=6 wt% calculated using approach Plank and Langmuir (1988).